Adsorption of Plasmid DNA to a Natural Organic Matter-Coated Silica Surface: Kinetics, Conformation, and Reversibility

Thanh H. Nguyen*,† and Menachem Elimelech‡

Department of Civil and Environmental Engineering, University of Illinois at Urbana-Champaign, 3230 Newmark Lab, Urbana, Illinois 61801, and Department of Chemical Engineering, Environmental Engineering Program, Yale University, New Haven, Connecticut 06520-8286

Received July 31, 2006. In Final Form: November 26, 2006

A quartz crystal microbalance with dissipation (QCM-D) has been used to determine the adsorption rate of ampicillin-resistant linear and supercoiled plasmid DNA onto a silica surface coated with natural organic matter (NOM). The structure of the resulting adsorbed DNA layer was determined by analyzing the viscoelastic properties of the adsorbed DNA layers as they formed and were then exposed to solutions of different ionic composition. The QCM-D data were complemented by dynamic light scattering measurements of diffusion coefficients of the DNA molecules as a function of solution ionic composition. The obtained results suggest that electrostatic interactions control the adsorption and structural changes of the adsorbed plasmid DNA on the NOM-coated silica surface. The adsorption of DNA molecules to the NOM layer took place at moderately high monovalent (sodium) electrolyte concentrations. A sharp decrease in solution ionic strength did not result in the release of the adsorbed DNA, indicating that DNA adsorption on the NOM-coated silica surface is irreversible under the studied solution conditions. However, the decrease in electrolyte concentration influenced the structure of the adsorbed layer, causing the adsorbed DNA to adopt a less compact conformation. The linear and supercoiled DNA had similar adsorption rates, but the linear DNA formed a thicker and less compact adsorbed layer than the supercoiled DNA.

1. Introduction

DNA immobilization on solid surfaces is a necessary step for DNA-based biosensors,[1−3] microarrays,[4,5] non-viral gene delivery, DNA hybridization,[6,7] protein−DNA interactions,[8] and DNA separation and purification using chromatographic columns. In non-viral gene delivery, a genetic material adsorbed onto a substrate is introduced into cells. The efficiency of gene delivery is therefore dependent on both the adsorption and detachment of the genetic materials. Because a significant amount of extracellular DNA is found in bacterial biofilms, DNA attachment to solid surfaces may also influence the formation and development of biofilms.[9] In the environment, extracellular DNA is present in soils, sediments, and natural waters on the order of a few micrograms of DNA per kilogram of soil/sediment or per liter of water.[10−19] Previous studies have shown that the adsorption of DNA to soil minerals protects DNA from enzymatic degradation, thus allowing for the subsequent transformation of competent bacteria.[20−24]

Microscopic techniques for studying DNA adsorption to solid surfaces include atomic force microscopy (AFM),[25−27] surface plasmon resonance,[28] low-temperature scanning electron microscopy (LTSEM),[29] and quartz crystal microbalance with dissipation (QCM-D).[6,7,30] AFM studies have focused on imaging DNA molecules adsorbed to a mica surface under different ionic compositions.[31,32] Even though these AFM studies have provided

* To whom correspondence should be addressed. Phone: 217-244-5965. Fax: 217-333-6968. E-mail: thn@uiuc.edu.

† University of Illinois at Urbana-Champaign.

‡ Yale University.

(1) Mannelli, F.; Minunni, A.; Tombelli, S.; Wang, R. H.; Spiriti, M. M.; Mascini, M. *Bioelectrochemistry* **2005**, *66*, 129−138.

(2) Pedano, M. L.; Rivas, G. A. *Biosens. Bioelectron.* **2003**, *18*, 269−277.

(3) Pedano, M. L.; Rivas, G. A. *Sensors* **2005**, *5*, 424−447.

(4) Pease, A. C.; Solas, D.; Sullivan, E. J.; Cronin, M. T.; Holmes, C. P.; Fodor, S. P. A. *Proc. Natl. Acad. Sci. U.S.A.* **1994**, *91*, 5022−5026.

(5) Schena, M.; Shalon, D.; Heller, R.; Chai, A.; Brown, P. O.; Davis, R. W. *Proc. Natl. Acad. Sci. U.S.A.* **1996**, *93*, 10614−10619.

(6) Hook, F.; Ray, A.; Norden, B.; Kasemo, B. *Langmuir* **2001**, *17*, 8305−8312.

(7) Larsson, C.; Rodahl, M.; Hook, F. *Anal. Chem.* **2003**, *75*, 5080−5087.

(8) Hansma, H. G.; Laney, D. E.; Bezanilla, M.; Sinsheimer, R. L.; Hansma, P. K. *Biophys. J.* **1995**, *68*, 1672−1677.

(9) Branda, S. S.; Vik, A.; Friedman, L.; Kolter, R. *Trends Microbiol.* **2005**, *13*, 20−26.

(10) Corinaldesi, C.; Danovaro, R.; Dell'Anno, A. *Appl. Environ. Microbiol.* **2005**, *71*, 46−50.

(11) Dell'Anno, A.; Corinaldesi, C. *Appl. Environ. Microbiol.* **2004**, *70*, 4384−4386.

(12) Dell'Anno, A.; Bompadre, S.; Danovaro, R. *Limnol. Oceanogr.* **2002**, *47*, 899−905.

(13) Danovaro, R.; Corinaldesi, C.; Dell'Anno, A.; Fabiano, M.; Corselli, C. *Environ. Microbiol.* **2005**, *7*, 586−592.

(14) Kroncke, I.; Stoeck, T.; Wieking, G.; Palojarvi, A. *Mar. Ecol.: Prog. Ser.* **2004**, *282*, 13−31.

(15) Maruyama, A.; Oda, M.; Higashihara, T. *Appl. Environ. Microbiol.* **1993**, *59*, 712−717.

(16) Jiang, S. C.; Paul, J. H. *Appl. Environ. Microbiol.* **1995**, *61*, 317−325.

(17) Deflaun, M. F.; Paul, J. H.; Davis, D. *Appl. Environ. Microbiol.* **1986**, *52*, 654−659.

(18) Agnelli, A.; Ascher, J.; Corti, G.; Ceccherini, M. T.; Nannipieri, P.; Pietramellara, G. *Soil Biol. Biochem.* **2004**, *36*, 859−868.

(19) Niemeyer, J.; Gessler, F. *J. Plant Nutr.* **2002**, *165*, 121−124.

(20) Cai, P.; Huang, Q. Y.; Zhang, X. W. *Environ. Sci. Technol.* **2006**, *40*, 2971−2976.

(21) Demaneche, S.; Jocteur-Monrozier, L.; Quiquampoix, H.; Simonet, P. *Appl. Environ. Microbiol.* **2001**, *67*, 293−299.

(22) Arderma, B. W.; Lorenz, M. G.; Krumbein, W. E. *Appl. Environ. Microbiol.* **1983**, 417−420.

(23) Demaneche, S.; Kay, E.; Gourbiere, F.; Simonet, P. *Appl. Environ. Microbiol.* **2001**, *67*, 2617−2621.

(24) Gallori, E.; Bazzicalupo, M.; Dalcanto, L.; Fani, R.; Nannipieri, P.; Vettori, C.; Stotzky, G. *FEMS Microbiol. Ecol.* **1994**, *15*, 119−126.

(25) Liu, Z. G.; Li, Z.; Zhou, H. L.; Wei, G.; Song, Y. H.; Wang, L. *Microsc. Res. Tech.* **2005**, *66*, 179−185.

(26) Ellis, J. S.; Abdelhady, H. G.; Allen, S.; Davies, M. C.; Roberts, C. J.; Tendler, S. J. B.; Williams, P. M. *J. Microsc. (Oxford)* **2004**, *215*, 297−301.

(27) Zheng, H. P.; Li, Z.; Wu, A. G.; Zhou, H. L. *Biophys. Chem.* **2003**, *104*, 37−43.

(28) Gong, H. F.; Garcia-Turiel, J.; Vasilev, K.; Vinogradova, O. I. *Langmuir* **2005**, *21*, 7545−7550.

(29) Poly, F.; Chenu, C.; Simonet, P.; Rouiller, J.; Monrozier, L. J. *Langmuir* **2000**, *16*, 1233−1238.

(30) Graneli, A.; Edvardsson, M.; Hook, F. *ChemPhysChem* **2004**, *5*, 729−733.

(31) Pastre, D.; Pietrement, O.; Fusil, P.; Landousy, F.; Jeusset, J.; David, M. O.; Hamon, C.; Le Cam, E.; Zozime, A. *Biophys. J.* **2003**, *85*, 2507−2518.

10.1021/la0622525 CCC: $37.00
Published on Web 02/08/2007

evidence of conformational changes of DNA molecules adsorbed to mica, no quantitative information was available. Hook et al.[6] and Larsson et al.[7] studied the interactions of single-strand DNA onto polymeric layers and subsequent DNA hybridization using QCM-D. These investigators applied the Voigt-based model to the QCM-D data to obtain information on the viscoelastic properties of each layer and the efficiency of DNA hybridization.

Studies that help one understand the fate and transport of DNA in natural environments have used clay, clay−humic acid complexes, and sand as model solid surfaces. For example, Poly et al.[29] used a combination of batch experiments and LTSEM to show that supercoiled plasmid DNA molecules form bridges between two clay platelets, while linear DNA molecules adsorb to edges of the clay platelet. Only two studies, both by Crecchio et al.,[33,34] have addressed the adsorption of DNA to humic acid and humic acid complexes. The focus of these two studies, however, was on the protection of DNA adsorbed to humic acid against degradation by DNase and the ability of the adsorbed DNA to transform competent bacteria. Systematic studies that elucidate the mechanisms of DNA interaction with natural organic matter (NOM) are not available. Because NOM covers most surfaces in the subsurface environment, understanding the DNA adsorption mechanisms to NOM-coated surfaces will help predict the persistence and mobility of extracellular DNA in the subsurface environment.

In this paper, we present a systematic investigation on the adsorption kinetics and reversibility of linear and supercoiled plasmid DNA onto a silica surface coated with NOM. A QCM-D was used to determine the DNA adsorption rate at different ionic strengths, as well as the detachment and structural (conformational) changes that occurred as the DNA adsorbed layers were exposed to solutions with lower ionic strengths. The QCM-D results were complemented by diffusion coefficient data obtained from dynamic light scattering (DLS) measurements. The QCM-D and DLS data were used to elucidate the adsorption mechanisms of plasmid DNA onto adsorbed NOM layers and the resulting conformations of the adsorbed DNA layers.

2. Materials and Methods

2.1. Chemicals and Reagents. Analytical grade NaCl, poly-L-lysine (PLL) hydrobromide (molecular weight of approximately 93 kDa), and HEPES buffer were purchased from Sigma. All electrolyte and HEPES buffer solutions were filtered through a 0.22 μm sterile cellulose acetate filter (Corning Inc., Corning, NY) and kept at 4 °C until use. Before use, the solutions were sonicated for 30 min to remove air bubbles and kept at 27 °C until being introduced into the QCM-D sensor chamber.

Suwannee River NOM was obtained from the International Humic Substances Society (IHSS, St. Paul, MN). The NOM solution was made by dissolving 54 mg of the Suwannee River NOM in 0.1 L of deionized (DI) water, after which it was stirred overnight and filtered through a 0.22 μm sterile cellulose acetate filter. Twenty milliliters of the NOM filtrate was mixed with 18 mL of 100 mM NaCl solution and 162 mL of DI water to make the final NOM solution in 10 mM NaCl. This NOM solution was filtered again and kept at 4 °C until use. The total organic carbon (TOC) of the filtered NOM solution was 21.83 ± 0.13 mg/L (duplicate measurements of 21.92 and 21.74 mg/L). All solutions were made using DI water with a resistivity of at least 18 MΩ.

2.2. Linear and Supercoiled Plasmid DNA Preparation. *E. coli* XL1 blue strains with the ampicillin-resistant plasmid vector pGEM-Teasy (3015 bp) were used as a source of plasmid DNA. A single colony from a freshly streaked plate was selected for inoculating 5 mL of starter culture into LB broth containing 0.1 mg/mL ampicillin. After 8 h of incubation, the starter culture was diluted into 5 L of ampicillin containing the LB broth for 12 h of incubation. The cell density in the final broth was approximately 10^9 per milliliter, as measured by optical density (SmartSpect 3000, Bio-Rad Laboratories, CA). Plasmid DNA extraction and purification was performed with the Qiagen EndoFree Plasmid Giga kits according to the protocol recommended by the company (Qiagen Inc. CA). After final DNA precipitation with 70% ethanol, the DNA precipitates were dissolved into 20 mL of DI water, which was purchased from American Bioanalytical (Natick, MA) and tested for RNase and endotoxins by the company. To facilitate DNA precipitate dissolution, the DI water was adjusted to pH 8 using 1 M NaOH.

To obtain the linear plasmid DNA, we performed enzymatic digestion for the extracted supercoiled plasmid DNA using the enzyme Nsi I (New England Biolabs, Inc., Beverly, MA). For enzymatic digestion, we divided 20 mL of supercoiled plasmid DNA solution into 20 1-mL aliquots stored in 2-mL microcentrifuge tubes. After the addition of 15 μL of Nsi I to each aliquot, the mixture was mixed, centrifuged for 1 min, and incubated at 37 °C for 14 h. After this incubation period, 10 μL of Nsi I was added to each aliquot followed by an incubation period of 1 h at 37 °C. Two microliters of the DNA mixture was then taken for agarose analysis to ensure complete digestion. Subsequently, 20 aliquots of digested DNA mixtures were combined. To purify the digested DNA, 160 mL of solution containing 750 mM NaCl and 50 mM MOPS at pH 7 was added to the combined 20 mL of DNA solution. Two QIAGEN−tip 10000s were used to purify 180 mL of this DNA solution, according to the manufacturer's recommendation. As with the supercoiled plasmid DNA, the final linear DNA precipitates with 70% ethanol were dissolved in 20 mL of DI water with a pH adjusted to 8. For both linear and supercoiled plasmid DNA, the DNA solution was divided into 200 μL aliquots and kept at −20 °C until use.

UV-absorbance spectra were obtained for both supercoiled and linear plasmid DNA using the NanoDrop ND-1000 spectrophotometer (NanoDrop Technologies, Wilmington, DE). To determine DNA concentration, we obtained a calibration curve using standard solutions of salmon sperm DNA at 10 mg/mL (Invitrogen). TE buffer containing 10 mM Tris HCl and 1 mM EDTA at pH 8 was used for the standard DNA solutions. The supercoiled and linear plasmid DNA solutions were diluted 100 times and 10 times, respectively, into the TE buffer to determine the DNA concentrations.

A supercoiled plasmid ladder (Invitrogen) and a 1-kb linear plasmid ladder (New England Biolabs, Inc.) were used to check the integrity of the extracted plasmid DNA. Twenty microliters of each ladder and plasmid DNA solution at 100× dilution were loaded into a 1% agarose gel. After 1 h of electrophoresis at 100 V, the agarose gel was stained with 20 mg/L ethidium bromide for 30 min before imaging with a gel documentation system (Bio-Rad Laboratories, CA).

2.3. Determination of Plasmid Diffusion Coefficients by DLS. A multidetector light-scattering unit (ALV-5000, Langen, Germany) with a Nd:vanadate (Nd:YVO_4) laser light source was used to determine plasmid diffusion coefficients. The DLS instrument and the measurement protocol have been described in detail in our recent work.[35] Briefly, all DLS measurements were obtained with the detector positioned at a scattering angle of 90°. For each measurement, the mixture was slowly transferred into the glass sample vials, which were closed with Teflon-lined caps. The concentration of the plasmid DNA for the DLS measurements was 114 mg/L. For each sample, 40 autocorrelation functions were obtained during the 600-s measurement. The scattered light intensity was approximately 30 kHz for all measurements.

2.4. QCM-D. Plasmid DNA adsorption kinetics and reversibility, as well as the viscoelastic properties of the adsorbed layers, were measured by the QCM-D D-300 system (Q-Sense AB, Gothenburg, Sweden). The crystals, with a fundamental resonant frequency of $f_0 \approx 5$ MHz, were coated with SiO_2 by vapor deposition and were

(32) Pietrement, O.; Pastre, D.; Fusil, S.; Jeusset, J.; David, M. O.; Landousy, F.; Hamon, L.; Zozime, A.; Le Cam, E. *Langmuir* **2003**, *19*, 2536−2539.
(33) Crecchio, C.; Stotzky, G. *Soil Biol. Biochem.* **1998**, *30*, 1061−1067.
(34) Crecchio, C.; Ruggiero, P.; Curci, M.; Colombo, C.; Palumbo, G.; Stotzky, G. *Soil Sci. Soc. Am. J.* **2005**, *69*, 834−841.
(35) Nguyen, T. H.; Elimelech, M. *Biomacromolecules* **2007**, *8*, 24−32.

supplied by Q-Sense (batch 051031). Before each measurement, the crystals were soaked overnight in a 2% Hellmanex II solution (Hellma GmbH & Co KG, Müllheim, Germany), rinsed thoroughly with DI water, dried with ultrahigh-purity N_2 gas, and treated for 30 min in a UV/O_3 chamber. The QCM-D experiments were performed in a flow-through mode, using a syringe pump (Kd Scientific, Inc., Holliston, MA) operating in withdrawal mode. Specifically, the pump was connected to the sensor crystal outlet and the studied solutions, contained within a syringe connected to the sensor crystal inlet, were fed through the crystal sensor chamber at a flow rate of 0.1 mL/min.

2.5. Protocol for Plasmid Adsorption Kinetics Studies. For each experiment in this study, the silica sensors were equilibrated for at least 30 min with a HEPES buffer made from 10 mM *N*-(2-hydroxyethyl)piperazine-*N*′-2-ethanesulfonic acid and 100 mM NaCl at an unadjusted pH of 5.8. After the equilibration period, the baselines of the frequency signals were stabilized at an approximately 2 Hz change in frequency over 1 h. The silica sensor was coated with NOM by the adsorption of a layer of PLL polycations onto the silica surface and subsequent adsorption of a layer of Suwannee River NOM. The layer of PLL was formed by flowing 2 mL of a PLL hydrobromide solution of 0.1 g/L in a HEPES buffer through the sensor chamber. At this pH condition, the PLL layer is positively charged because of the amine groups. The PLL layer was rinsed with the HEPES buffer for 20 min and with 10 mM NaCl for another 20 min. After this 40-min washing, the PLL layer was covered by a layer of NOM formed by flowing 2 mL of Suwannee River NOM solution at 21 mg/L TOC through the sensor chamber. This NOM layer was then washed with 10 mM NaCl solution and a DNA-free electrolyte solution of the same ionic composition to be used in subsequent DNA adsorption experiments. Each rinse lasted for 20 min. After the formation of the NOM layer on the silica sensor and subsequent washing, plasmid DNA experiments were conducted by flowing the following solutions through the sensor chamber: 4 mL of plasmid DNA solution at 120 mg/L concentration in a particular electrolyte solution (step 1), 2 mL of DNA-free electrolyte solution (step 2), 2 mL of 10 mM NaCl solution (step 3), 2 mL of 1 mM NaCl solution (step 4), and 2 mL of DI water (step 5). Step 1 was used for studying the adsorption kinetics of plasmid DNA onto the NOM layer. Step 2 was a rinsing step. Steps 3−5 were for the study of adsorption reversibility and the structural changes of plasmid DNA layers as a function of solution composition. All experiments were conducted in duplicate.

Experiments with DNA-free electrolyte solutions were also performed to check the sensitivity of the quartz crystal vibration to changes in ionic strengths. Specifically, after the formation of PLL and subsequent NOM layers, each of the following solutions were sequentially pumped through the crystal chamber for 20 min: 100 mM or 300 mM NaCl, 10 mM NaCl, 1 mM NaCl, and DI water. The changes in frequency and dissipation observed in these experiments will be referred to as the "buffer effect" for DNA-free experiments.

2.6. QCM-D Data Analysis. For adsorption experiments, the adsorption rate was estimated as the initial slope of the change in frequency $f_{(3)}$ versus time curve. A favorable (nonrepulsive) adsorption condition was created by adsorbing a layer of PLL onto the silica sensor. After rinsing the PLL layer with HEPES buffer and 10 mM NaCl, as described above, 2 mL of plasmid DNA solution at a 120 mg/L concentration in 10 mM NaCl solution was introduced into the sensor chamber. The adsorption rates for favorable conditions were 14.5, 15.6, and 17.9 Hz/min (average 16.0 ± 1.7 Hz/min) for supercoiled plasmid DNA, and 17.4 and 16.6 Hz/min (average 17.0 ± 0.6 Hz/min) for linear DNA. The attachment efficiency (α), also known as the inverse stability ratio (1/*W*), for each experiment was then calculated as the ratio of the actual rate divided by the corresponding average of the adsorption rate at favorable conditions (i.e., 16.0 Hz/min for supercoiled plasmid DNA and 17.0 Hz/min for linear DNA).

The viscosity and thickness of the adsorbed layers were estimated using a viscoelastic model based on the Voigt model, as presented in the works of Voinova et al.[36] Briefly, in this model, the shear viscosity (η), shear modulus (μ), and Voigt thickness (d_{Voigt}) of the adsorbed layer were obtained by modeling the experimental data of Δf and ΔD for at least two overtones using the program Q-Tools provided by Q-Sense AB. This program applies a curve-fitting algorithm that searches for the unknown parameters (η, μ, d_{Voigt}) by minimizing the χ^2 parameter. Besides the experimental data of Δf and ΔD for at least two overtones, this model requires the solution density (1000 kg/m^3) and viscosity (10^{-3} Pa s), and the density of the adsorbed layer (1030 kg/m^3), following the recommendations of Gurdak et al.[37] Modeling was performed using the same initial parameters for four combinations of experimental data collected at different overtones (i.e., $n = 3,5$; $n = 3,7$; $n = 5,7$; and $n = 3,5,7$). The fitting results were qualitatively similar for all cases, indicating that the viscoelastic properties were frequency independent. Fitted parameters were forced between maximal and minimal guesses for viscosity (10^{-5}, 10^{-2} Pa s), shear modulus (10^3, 3×10^6 Pa), and Voigt thickness of the adsorbed layer (0.1, 25 nm). A similar modeling approach for the adsorbed DNA layer was applied successfully by Stengel et al.[38] In our study, the changes in frequency and dissipation were also monitored continuously from the formation of the PLL layer throughout the rinsing by DI water. Modeling was performed, however, only for the data obtained after the formation of the NOM layer (i.e., steps 1−5 for plasmid DNA adsorption). In addition, at the beginning of step 1, frequency, dissipation, and time were set to zero so that the changes in frequency and dissipation monitored during steps 1−5 reflect the adsorption of plasmid DNA onto the NOM layer.

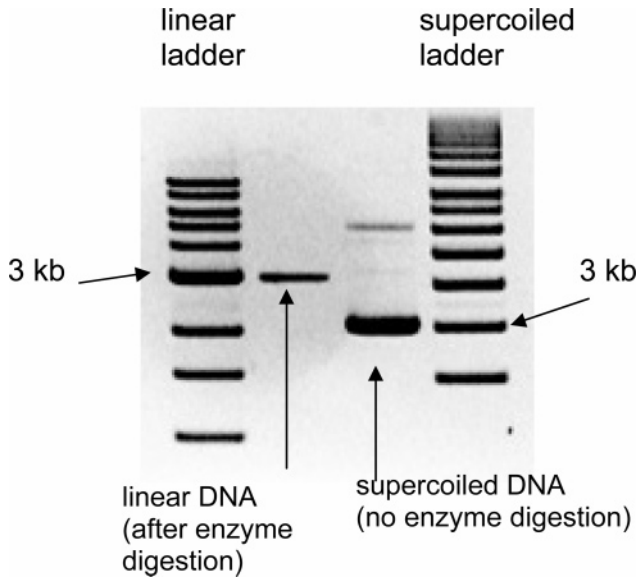

Figure 1. Agarose gel electrophoresis image of plasmid pGEM-Teasy. The first lane is the linear ladder. The second lane is the linear DNA after enzyme digestion of the plasmid and subsequent purification. The third lane is the plasmid before enzyme digestion; here, the major dark band, at 3 kb, shows the supercoiled form of the plasmid, while the minor thin band, around 7.5 kb, shows the relaxed form of the plasmid. The fourth lane is the supercoiled ladder.

3. Results and Discussion

3.1. Plasmid DNA Characterization. The linear form of the digested plasmid DNA shows a single broadband at 3 kb (lane 2, Figure 1). For the undigested plasmid DNA, two bands were observed in the agarose gel (lane 3, Figure 1): a broadband at

(36) Voinova, M. V.; Rodahl, M.; Jonson, M.; Kasemo, B. *Phys. Scr.* **1999**, *59*, 391−396.
(37) Gurdak, E.; Dupont-Gillain, C. C.; Booth, J.; Roberts, C. J.; Rouxhet, P. G. *Langmuir* **2005**, *21*, 10684−10692.
(38) Stengel, G.; Hook, F.; Knoll, W. *Anal. Chem.* **2005**, *77*, 3709−3714.

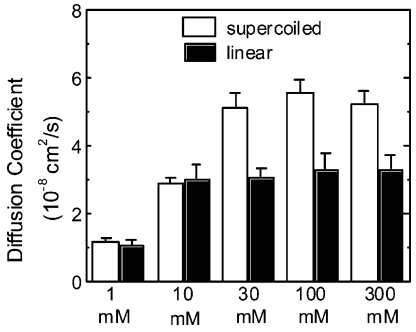

Figure 2. Diffusion coefficients of plasmid DNA in monovalent salt solutions at ambient pH (pH 5.8). The presented data are averages and standard deviations for 40 measurements of a single sample. Plasmid DNA concentrations during the measurements were 114 mg/L, and the temperature was 23 °C. The error bars represent one standard deviation.

3 kb and a much smaller band at around 7.5 kb. Thus, we conclude that the vast majority of the extracted and undigested plasmid is in the supercoiled form, and that only the linear form of DNA exists in the digested plasmid. The A260/A280 ratios for the plasmid DNA solutions were 1.8, indicating that the plasmid DNA solutions were not contaminated by proteins.[39,40]

3.2. Influence of Ionic Strength on Plasmid Diffusion Coefficients. Figure 2 shows diffusion coefficients for supercoiled and linear plasmid DNA in solutions with different ionic strengths. Over the range of studied ionic strengths from 30 to 300 mM NaCl, linear plasmid DNA molecules have lower diffusion coefficients than supercoiled plasmid DNA. Because linear plasmid DNA molecules have a more flexible conformation than supercoiled DNA, it is expected that linear plasmid DNA would be larger in size and, therefore, have lower diffusion coefficients than supercoiled plasmid DNA. Seils and Pecora[41] reported similar observations. For a 2.3 kbp plasmid DNA in a solution of 100−200 mM NaCl, they reported diffusion coefficients for the relaxed circular and linear plasmid DNA of 4.79×10^{-8} and 4.42×10^{-8} cm^2/s, respectively.

For both supercoiled and linear plasmid DNA, the diffusion coefficients increase with ionic strength. Specifically, in a 1 mM NaCl solution, diffusion coefficients are smallest at $1.21 \pm 0.09 \times 10^{-8}$ cm^2/s (supercoiled DNA) and $1.13 \pm 0.09 \times 10^{-8}$ cm^2/s (linear DNA). In a 10 mM NaCl solution, these values increase to $2.90 \pm 0.17 \times 10^{-8}$ cm^2/s (supercoiled DNA) and $3.07 \pm 0.39 \times 10^{-8}$ cm^2/s (linear DNA). The diffusion coefficients are highest and statistically the same in 100 mM and 300 mM NaCl solutions (Figure 2). The observed positive correlation between the diffusion coefficients of plasmid DNA and solution ionic strength can be explained by electrostatic interactions among subunits of the plasmid DNA molecules. In monovalent salt solutions, Na^+ screens negative charges along the phosphate backbone of the plasmid DNA molecules. As the Na^+ concentration increases, charge screening is more pronounced, leading to reduced electrostatic repulsion among subunits of plasmid DNA molecules. As a result, subunits of the plasmid DNA can come closer to each other, thus resulting in smaller, more compact plasmid DNA molecules with higher diffusion coefficients.

Liu et al.[42] observed a positive correlation between diffusion coefficients and ionic strengths for three linear plasmids. For example, for a 1.5 kbp plasmid, the diffusion coefficient increased from $5.25 \pm 0.37 \times 10^{-8}$ cm^2/s in 0.1 mM NaCl solution to $6.93 \pm 0.21 \times 10^{-8}$ cm^2/s in 8 mM NaCl solution.[42] For a 2.3 kbp plasmid, the diffusion coefficient increased from $4.07 \pm 0.30 \times 10^{-8}$ cm^2/s in 3 mM NaCl solution to $4.92 \pm 0.39 \times 10^{-8}$ cm^2/s in 27 mM NaCl solution.[42] Therefore, our results are consistent with the findings of Liu et al.[42] discussed above. In addition, our results are consistent with published data by Seils and Pecora.[41] For example, for a 2.3 kbp linear plasmid DNA in 100 mM NaCl, they reported a diffusion coefficient of 4.42×10^{-8} cm^2/s. For the larger 3 kbp linear plasmid DNA used in our study, the diffusion coefficient is 4.95×10^{-8} cm^2/s.

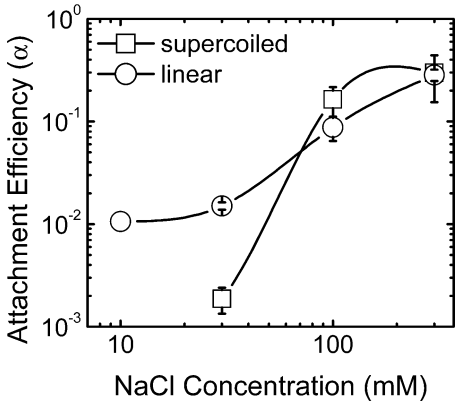

Figure 3. Adsorption kinetics of plasmid DNA onto silica surfaces coated with NOM at ambient pH (pH 5.8) at different solution ionic strengths. Adsorption rates were taken as the initial slopes of the curves of normalized frequency shift at the third overtone ($\Delta f_{(3)}$) vs time. Attachment efficiency is obtained by normalizing the actual plasmid adsorption rate by the favorable adsorption rate on a PLL-coated silica surface layer (-16.0 ± 1.7 Hz/min for supercoiled DNA and -17.0 ± 0.6 Hz/min for linear DNA). Shown are average values of at least two replicate measurements. Error bars indicate standard deviations. The plasmid concentrations during the experiments were 120 mg/L, and the temperature was 25 °C.

3.3. Kinetics of Plasmid DNA Adsorption. As described earlier, a layer of NOM was deposited on top of a layer of positively charged PLL. When a 120 mg/L solution of supercoiled plasmid DNA in 10 mM ionic strength was flowed through the QCM-D chamber after the sequential deposition of PLL and NOM layers, the variations in frequency and dissipation were 0.2 Hz and 0.1×10^{-5}, respectively, over 40 min. Because these variations are similar to the baseline fluctuations, we conclude that no supercoiled plasmid DNA deposited onto the NOM layer under these conditions. This observation also proves that the positively charged PLL layer was completely covered by the NOM layer. If the PLL layer was not covered completely by the NOM layer, deposition of negatively charged DNA molecules onto the regions of the uncovered positively charged PLL layer would occur, and significant variation in frequency and dissipation would be measurable.

Figure 3 presents the attachment efficiencies for supercoiled and linear plasmid DNA at different ionic strengths. The results demonstrate that, as the ionic strengths increase, the attachment efficiencies also increase. At 10 and 30 mM ionic strength, the attachment efficiencies for linear plasmid DNA are 0.01 and 0.015, respectively. For supercoiled plasmid DNA, no deposition was observed at 10 mM ionic strength (i.e., below the detection limit of the QCM-D), and the attachment efficiency at 30 mM ionic strength was about 10 times lower than that for linear plasmid DNA. At 100 and 300 mM ionic strength, the attachment efficiencies increased to 0.16 and 0.30 for supercoiled plasmid DNA, and 0.09 and 0.28 for linear plasmid DNA. While the

(39) Wilfinger, W. W.; Mackey, K.; Chomcynski, P. *BioTechniques* **1997**, *22*, 474−481.
(40) Manchester, K. L. *BioTechniques* **1995**, *19*, 208−210.
(41) Seils, J. C.; Pecora, R. *Macromolecules* **1992**, *25*, 354−362.
(42) Liu, H.; Gapinski, J.; Skibinska, L.; Patkowski, A.; Pecora, R. *J. Chem. Phys.* **2000**, *113*, 6001−6010.

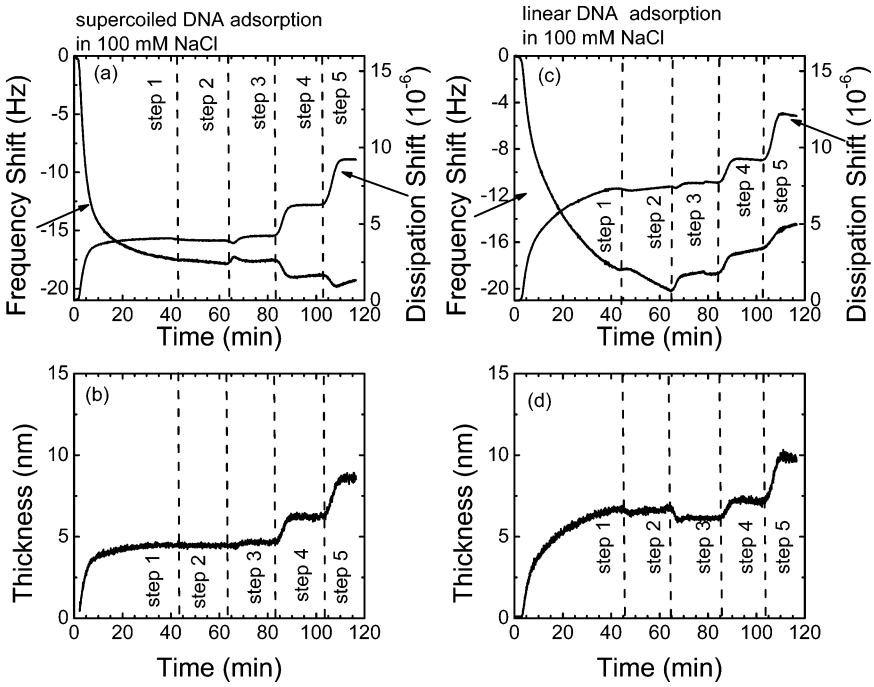

Figure 4. (a) Frequency shift divided by the third harmonic number ($\Delta f_{(3)}$) and associated dissipation shifts (ΔD_3) as a function of time for supercoiled plasmid adsorption at ambient pH (pH 5.9). The plasmid concentration was 120 mg/L, and the plasmid adsorption took place in 100 mM NaCl (step 1). The adsorbed supercoiled plasmid layer was rinsed with 100 mM NaCl (step 2), 10 mM NaCl (step 3), 1 mM NaCl (step 4), and DI water (step 5). (b) Changes in thickness of the adsorbed supercoiled DNA layer. (c) Frequency shift divided by the third harmonic number ($\Delta f_{(3)}$) and associated dissipation shifts (ΔD_3) as a function of time for linear plasmid adsorption at ambient pH (pH 5.9). The plasmid concentration was 120 mg/L, and the plasmid adsorption took place in 100 mM NaCl (step 1). The adsorbed plasmid layer was rinsed with 100 mM NaCl (step 2), 10 mM NaCl (step 3), 1 mM NaCl (step 4), and DI water (step 5). (d) Changes in thickness of the adsorbed linear DNA layer. For supercoiled DNA adsorption in 100 mM NaCl (Figure 4b), the thickness data for the first 2 min are omitted (see discussion in text). Note that only data for one run are presented for clarity.

attachment efficiencies for supercoiled plasmid DNA are 10 times lower than those for linear plasmid DNA at low ionic strengths, the attachment efficiencies for both forms of plasmid DNA are similar at higher ionic strengths.

The trend in attachment efficiencies as a function of ionic strength can be explained by electrostatic double-layer repulsion between the DNA and the NOM layer. At ambient pH conditions (pH 5.8), DNA and NOM molecules are negatively charged. As the ionic strength increases, charge shielding by Na^+ for both NOM and DNA molecules increases. Consequently, the interactions between DNA and NOM molecules become less repulsive. At the highest ionic strength studied (i.e., 300 mM), adsorption rates for both forms of plasmid DNA are comparable, and are about 30% of those under favorable (nonrepulsive) conditions.

The observation that, at low ionic strength, the linear DNA has a higher attachment efficiency than supercoiled DNA may be attributable to their conformations. At low ionic strengths, with significant electrostatic repulsion among subunits of the DNA molecules, linear DNA molecules are expected to have an extended conformation. It is possible that the ends of the extended linear DNA molecules can approach the NOM layer more effectively than the supercoiled form of DNA. Romanowski et al.[43] reported similar observations that linear DNA molecules adsorbed more to sand than supercoiled DNA molecules. At high ionic strengths, both forms of plasmid DNA have more compact conformations, as discussed above, which results in similar adsorption rates. In addition, at high ionic strengths, the energy barrier to deposition is significantly reduced or may even disappear, allowing both forms of plasmid DNA to adsorb to the NOM layer at comparable rates.

(43) Romanowski, G.; Lorenz, M. G.; Wackernagel, W. *Appl. Environ. Microbiol.* **1991**, *57*, 1057−1061.

3.4. Reversibility of Adsorbed DNA. Figures 4a,c and 5a,c show variations in frequency and dissipation during plasmid DNA adsorption in either 100 or 300 mM NaCl and subsequent exposure of the adsorbed layer to solutions with lower ionic strengths (i.e., 10 mM NaCl, 1 mM NaCl, and DI water). For all cases, when the electrolyte solutions were switched from either 100 or 300 mM NaCl to 10 mM NaCl (step 3), the frequency $\Delta f_{(3)}$ increases by up to 3.6 ± 0.3 Hz (Figure 5a, layer of supercoiled plasmid formed in 300 mM NaCl). This increase in frequency $\Delta f_{(3)}$ does not indicate DNA detachment from the NOM layer, but rather reflects the so-called "buffer effect" that occurred in DNA-free solution experiments, in which we observed that $\Delta f_{(3)}$ increases by 4.7 Hz when the electrolyte solution was changed from 300 to 10 mM NaCl.

When the electrolyte solution flowing through the adsorbed DNA layer was switched from 10 to 1 mM NaCl (step 4), a decrease in frequency by 1.1 ± 0.2 or 1.8 ± 0.8 Hz and an increase in dissipation by $(2.5 \pm 0.5) \times 10^{-6}$ or $(2.3 \pm 0.3) \times 10^{-6}$ (Figures 4a and 5a) were observed for the supercoiled DNA layer formed in 100 or 300 mM NaCl, respectively. Similarly, when the linear DNA layer formed in 300 mM NaCl was exposed to 1 mM NaCl, frequency decreased by 1.5 ± 0.7 Hz and dissipation increased by $(3.5 \pm 0.1) \times 10^{-6}$ (step 4, Figure 5c). For the DNA-free solution experiments, switching solutions from 10 to 1 mM resulted in an increase of 0.7 Hz in frequency and a decrease of 0.1×10^{-6} for dissipation. Note that the change in frequency and dissipation observed during step 4 in Figures 4a and 5a,c was in the opposite direction and significantly higher than the variations observed in DNA-free solution experiments. We therefore conclude that the buffer effects during step 4 are not likely to significantly influence the observed results with regards to the adsorbed DNA layer on the NOM-coated surface.

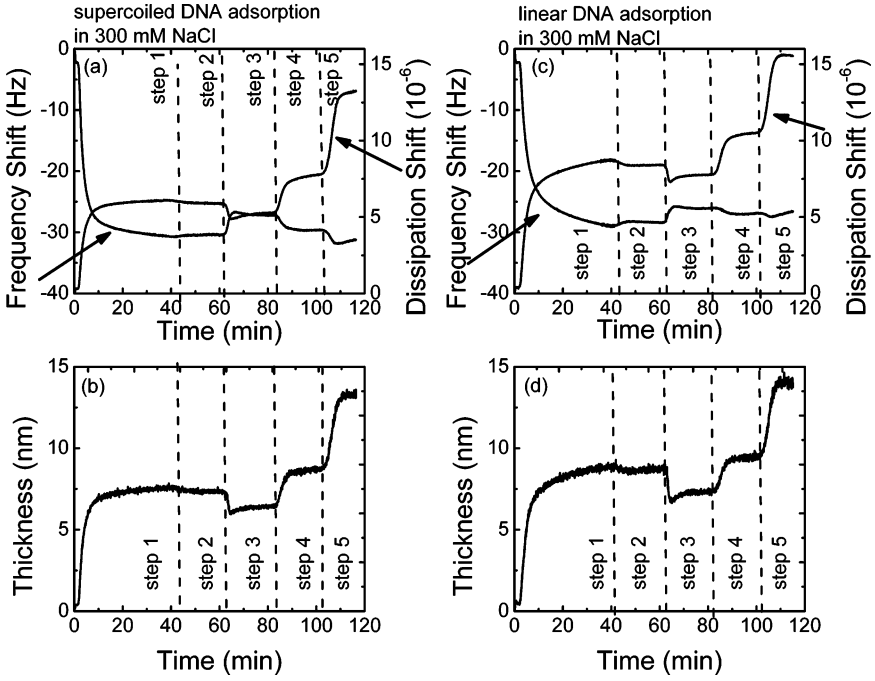

Figure 5. (a) Frequency shift divided by the third harmonic number ($\Delta f_{(3)}$) and associated dissipation shifts (ΔD_3) as a function of time for supercoiled plasmid adsorption at ambient pH (pH 5.9). The plasmid concentration was 120 mg/L, and the plasmid adsorption took place in 300 mM NaCl (step 1). The adsorbed supercoiled plasmid layer was rinsed with 100 mM NaCl (step 2), 10 mM NaCl (step 3), 1 mM NaCl (step 4), and DI water (step 5). (b) Changes in thickness of the adsorbed supercoiled DNA layer. (c) Frequency shift divided by the third harmonic number ($\Delta f_{(3)}$) and associated dissipation shifts (ΔD_3) as a function of time for linear plasmid adsorption at ambient pH (pH 5.9). The plasmid concentration was 120 mg/L, and the plasmid adsorption took place in 300 mM NaCl (step 1). The adsorbed plasmid layer was rinsed with 300 mM NaCl (step 2), 10 mM NaCl (step 3), 1 mM NaCl (step 4), and DI water (step 5). (d) Changes in thickness of the adsorbed linear DNA layer. Note that only data for one run are presented for clarity.

Table 1. Best Fittings for Shear Viscosity, Shear Modulus, and Effective Thickness as Obtained Using the Voigt-Based Model[a]

ionic composition	viscosity (10^{-3} Pa s)	shear modulus (10^5 Pa)	effective thickness (nm)
supercoiled plasmid DNA			
adsorption in 100 mM NaCl	1.44; 1.42	1.66; 1.65	4.4; 4.5
rinsing with 100 mM NaCl	1.48; 1.46	1.76; 1.79	4.5; 4.6
rinsing with 10 mM NaCl	1.40; 1.41	1.62; 1.74	4.6; 4.9
rinsing with 1 mM NaCl	1.24; 1.24	1.19; 1.26	6.1; 6.4
rinsing with DI water	1.14; 1.12	0.93; 0.89	8.1; 9.0
adsorption in 300 mM NaCl	1.72; 1.65	2.28; 1.97	5.7; 7.4
rinsing with 300 mM NaCl	1.77; 1.68	2.37; 2.02	5.8; 7.4
rinsing with 10 mM NaCl	1.79; 1.69	2.83; 2.28	4.9; 6.5
rinsing with 1 mM NaCl	1.53; 1.49	2.11; 1.70	5.6; 8.0
rinsing with DI water	1.24; 1.32	1.15; 1.20	9.0; 10.9
linear plasmid DNA			
adsorption in 100 mM NaCl	1.17; 1.17	1.01; 0.89	6.1; 6.2
rinsing with 100 mM NaCl	1.20; 1.19	1.13; 0.94	6.6; 6.4
rinsing with 10 mM NaCl	1.15; 1.15	1.20; 0.94	6.1; 6.3
rinsing with 1 mM NaCl	1.08; 1.08	0.92; 0.72	7.2; 7.4
rinsing with DI water	1.03; 1.02	0.71; 0.55	9.7; 10.6
adsorption in 300 mM NaCl	1.48; 1.39	1.30; 1.33	11.3; 8.6
rinsing with 300 mM NaCl	1.48; 1.40	1.34; 1.33	11.2; 8.7
rinsing with 10 mM NaCl	1.42; 1.36	1.03; 1.48	12.1; 7.2
rinsing with 1 mM NaCl	1.31; 1.24	0.85; 1.12	14.9; 9.2
rinsing with DI water	1.22; 1.13	0.72; 0.84	20.4; 13.3

[a] The Voigt-based model was used for a single layer with a fixed density of 1030 kg/m^3 in all cases. Shown values are the average of all values collected as follows: plasmid adsorption, rinse in either 100 or 300 mM NaCl (step 2), rinse in 10 mM NaCl (step 3), rinse in 1 mM NaCl (step 4), and rinse in DI water (step 5). The two values for duplicate experiments are shown in each column. The first and second numbers in each column are the values obtained from the first and second experiment, respectively.

The combined decrease in frequency and increase in dissipation clearly indicates that no adsorbed plasmid DNA was detached from the NOM layer when the DNA layer was exposed to 1 mM NaCl.

Similar observations can be reported for step 5, when the supercoiled adsorbed DNA layers formed in 100 or 300 mM NaCl (Figures 4a and 5a) or the linear DNA layer formed in 300 mM NaCl (Figure 5c) were exposed to DI water. Specifically, for these cases, frequency decreased initially and then increased slightly (0.8 ± 1.1) Hz, but dissipation increased by up to (5.3 ± 0.4) $\times 10^{-6}$. Again, these changes are not due to the buffer effects in DNA-free solution experiments, because switching the electrolyte solution from 1 mM NaCl to DI water resulted in only a 0.1 Hz increase in frequency and immeasurable change in dissipation. Thus, the adsorbed plasmid DNA layers were stable even when they were exposed to DI water under the studied conditions.

Interesting phenomena were observed for the adsorbed linear DNA layer formed in 100 mM NaCl (Figure 4c). Subsequent exposure of the adsorbed DNA layer to 1 mM NaCl and DI water resulted in a significant increase in both frequency and dissipation. Specifically, frequency increased by 2.0 ± 0.6 and 1.7 ± 0.6 Hz during steps 4 and 5, respectively. The accompanied dissipation increased by (1.7 ± 1.2) $\times 10^{-6}$ and (2.1 ± 1.1) $\times 10^{-6}$ during steps 4 and 5, respectively. An increase in frequency and an accompanied decrease in dissipation indicate mass detachment. Increases in both frequency and dissipation suggest substantial softening of the adsorbed layer. This phenomenon was observed and theoretically predicted previously.[30,44] The evidence and discussion on DNA layer softening will be addressed in the next section. In addition, thicker layers of adsorbed DNA during

(44) Lucklum, R.; Behling, C.; Hauptmann, P. *Anal. Chem.* **1999**, *71*, 2488−2496.

exposure to 1 mM NaCl and DI water (steps 4 and 5 in Figure 4d) also suggest the lack of DNA detachment from the NOM layer, because DNA detachment should result in a thinner DNA adsorbed layer. Therefore, we again observed adsorption irreversibility for the adsorbed DNA layer onto the NOM layer.

3.5. Structure of Adsorbed Plasmid DNA. Table 1 presents the thickness, viscosity, and shear modulus of the adsorbed plasmid DNA layers that formed in solutions of either 100 or 300 mM NaCl, and were subsequently exposed to 10 mM NaCl, 1 mM NaCl, and DI water. Note that, for the adsorption step, the parameters for each run are presented as averages of data obtained when the layer is stable (i.e., from 17 min to approximately 45 min). In some cases, the Voigt-based model did not work for the first few minutes of plasmid adsorption, as the modeling results showed unexplainable spikes. For example, in the case of linear plasmid DNA adsorption in 100 mM NaCl, viscosity increased rapidly from 0.93×10^{-3} Pa s at 0.2 min to 1.3×10^{-3} Pa s at 2.6 min, decreased to 0.6×10^{-3} Pa s at 3.1 min, increased to 1.06×10^{-3} Pa s at 4.8 min, then increased slowly to 1.2×10^{-3} Pa s at 46 min. Therefore, we only report here the viscoelastic parameters obtained with the stable frequency and dissipation shift (from 17 min to approximately 45 min).

The adsorbed supercoiled DNA layers have lower thickness, higher viscosity, and larger shear modulus than the adsorbed linear DNA layers (Table 1), despite their similar adsorption rate (Figure 3). Because the adsorption rates were estimated based on the initial slope of the frequency curve, the conformation and fluidity of the DNA layer were not taken into account. In contrast, the thickness, viscosity, and shear modulus of the DNA layers were determined using a viscoelastic model that used frequency and dissipation data collected for at least two overtones. Because supercoiled plasmid DNA molecules are less flexible than those of linear plasmid DNA, it is expected that the adsorbed supercoiled DNA layers are more compact and therefore thinner, with higher viscosity than the adsorbed linear DNA layers.

The thinner layers formed in 100 mM NaCl have lower viscosity than the thicker layers formed in 300 mM NaCl ($(1.43 \pm 0.02) \times 10^{-3}$ Pa s versus $(1.69 \pm 0.04) \times 10^{-3}$ Pa s for supercoiled, and $(1.17 \pm 0.0) \times 10^{-3}$ Pa s versus $(1.43 \pm 0.06) \times 10^{-3}$ Pa s for linear, Table 1, average $\pm$ standard deviation of two runs). The combination of thinner and less viscous DNA layers suggests that the DNA layers formed in 100 mM NaCl are significantly softer and less compact than those formed in 300 mM NaCl. This fact is consistent with the expected influence of ionic strength on the DNA conformation as discussed above. As ionic strength increases, charge screening by the salt counterions is reduced, and electrostatic repulsion between subunits of the DNA decreases, leading to a more compact DNA conformation.

In all cases, as the ionic strength was decreased, the thickness of the adsorbed plasmid DNA layers increased, while their viscosity and shear modulus decreased. For example, for plasmid DNA layers formed in 100 mM NaCl, thickness increased from 4.4 ± 0.1 to 6.2 ± 0.3 nm (supercoiled DNA) and from 6.2 ± 0.3 to 7.3 ± 0.2 nm (linear DNA), when the layers were exposed to 1 mM NaCl, and subsequently to 8.6 ± 0.6 and 10.1 ± 0.7 nm, for supercoiled DNA and linear DNA, respectively, when the layers were exposed to DI water (Table 1, first run). The viscosity of the plasmid DNA layer formed in 100 mM NaCl decreased from $(1.43 \pm 0.02) \times 10^{-3}$ to $(1.24 \pm 0.0) \times 10^{-3}$ Pa s (for supercoiled) and from $(1.18 \pm 0.0) \times 10^{-3}$ to $(1.08 \pm 0.0) \times 10^{-3}$ Pa s (for linear) when the layers were exposed to 1 mM NaCl, and subsequently to $(1.13 \pm 0.0) \times 10^{-3}$ Pa s (for supercoiled) and $(1.03 \pm 0.0) \times 10^{-3}$ Pa s (for linear) when the layers were exposed to DI water (Table 1, first run). This observation can be explained by increased "softness" of the adsorbed layer due to lower electrostatic repulsion between subunits of DNA molecules in high ionic strength solutions. Note that when the adsorbed linear DNA layers that were formed in 100 mM NaCl were exposed to 1 mM NaCl and then to DI water, their viscosity reduced to $(1.13 \pm 0.0) \times 10^{-3}$ Pa s and $(1.03 \pm 0.0) \times 10^{-3}$ Pa s, respectively. The fact that the viscosity of the adsorbed linear DNA layers was close to that of water at 25 °C (i.e., 1.0×10^{-3} Pa s) indicates that the adsorbed linear DNA layers become substantially soft. In fact, these layers were so soft that the frequency of vibration increased as if there was measurable mass loss (Figure 4c).

As discussed in section 3.2, with less electrostatic repulsion among subunits of DNA molecules in lower ionic strength solutions, plasmid DNA molecules have less compact conformation, larger size, and higher diffusion coefficients (Figure 2). This trend is in agreement with the observed combination of decreased viscosity and increased thickness of the adsorbed plasmid DNA layers when the layers formed in either 100 mM or 300 mM NaCl are exposed to lower ionic strength solutions (i.e., 10 mM, 1 mM NaCl, and DI water). In summary, electrostatic interactions control the adsorption and structural changes of the adsorbed plasmid DNA onto a silica surface covered with NOM.

4. Concluding Remarks

Plasmid DNA adsorption to a silica surface covered with NOM was found to be significant under solution ionic strengths that are relevant to aquatic environments. Specifically, the attachment efficiency (α) ranged from 0.01 at 1 mM ionic strength for linear DNA to 0.3 at 300 mM ionic strength for both supercoiled and linear DNA. When the adsorbed DNA layers were exposed to solutions with lower ionic strengths (i.e., 1 mM NaCl and DI water), no DNA release was observed. These results suggest that, in subsurface environments, extracellular DNA can adhere to solid surfaces covered with NOM, and a sudden change in solution ionic strength, such as after rain events, does not lead to the release of adsorbed DNA from the surface. In addition, lowering ionic strength leads to a less compact adsorbed DNA layer. The results of this study on the adsorption kinetics and irreversibility suggest that intracellular DNA can exist in soil as a source of genetic material for natural transformation in bacteria.

Acknowledgment. Funding was provided by the Yale Institute for Biospheric Studies and the National Science Foundation (BES 0228911). We would like to thank Dr. Paul Van Tassel for letting us use the QCM-D, Dr. Barbara Kazmierczak for providing the bacterial strain, and Kai Loon Chen for the DLS experiments.

LA0622525